J. Fluid Mech. (1979), *vol.* 95, *part* 2, *pp.* 209–222
Printed in Great Britain

On the generation of viscous toroidal eddies in a cylinder

By J. R. BLAKE†

CSIRO Division of Mathematics and Statistics, PO Box 1965,
Canberra City, ACT, 2601, Australia

(Received 20 March 1979)

The streamlines due to a stokeslet on the axis in a finite, semi-infinite and infinite cylinder are obtained together with the case of a Stokes-doublet and source-doublet in an infinite cylinder. In the infinite and semi-infinite cylinder examples an infinite set of toroidal eddies are obtained. The eddies alternate in sign and the magnitude of the stream function decays exponentially with distance from the driving singularity. In the finite cylinder a primary interior eddy adjacent to the singularity is always obtained and, depending on location of the singularity within the cylinder and the ratio of cylinder length to radius, a finite number of secondary interior eddies. In the case of long cylinders, the eddies are generated along the axis, whereas, for squat cylinders, secondary eddies occur in the radial direction. The interior eddies emerge from the corner as the length of the cylinder is increased. Moffatt corner eddies exist but they are very much smaller than the interior eddies.

1. Introduction

The study of flow fields where inertial forces are negligible in comparison to viscous forces, known as *Stokes flow*, is becoming increasingly important in areas of biology, medicine, engineering, physics and chemistry. This flow regime is characterized by a very small numerical value for the Reynolds number R, defined as

$$R = \rho UL/\mu \ll 1, \tag{1}$$

where ρ is the density and μ the dynamic viscosity of the ambient fluid and U and L are characteristic velocity and length scales respectively. Two principal cases exist where we obtain very small values of R; they are when (*a*) we have a very viscous fluid (e.g. tar) or (*b*) the length and relative velocity scales are very small (e.g. red blood cells, micro-organisms, suspensions of small particles).

Often we need to study the resulting flow field due to the movement of a 'particle' near a boundary. To date, most mathematical analysis has been concerned with 'infinite' fluids, that is infinite in all directions, while a limited amount of analysis has been directed towards 'half-space' or infinite cylinder problems (see, for example, Happel & Brenner 1965; Aderogba 1976; Blake 1971). Theoretical modelling of flow fields generated in either semi-infinite or finite cylinders has generally received scant attention in the literature until recently.

Many practical problems involve the slow motion of particles near cylindrical boundaries which are either infinite, semi-infinite or finite in extent. Some examples are the motion of red blood cells in arterioles, capillaries and venules, sedimentation

† Present address: Department of Mathematics, University of Wollongong, P.O. Box 1144, NSW, 2500, Australia.

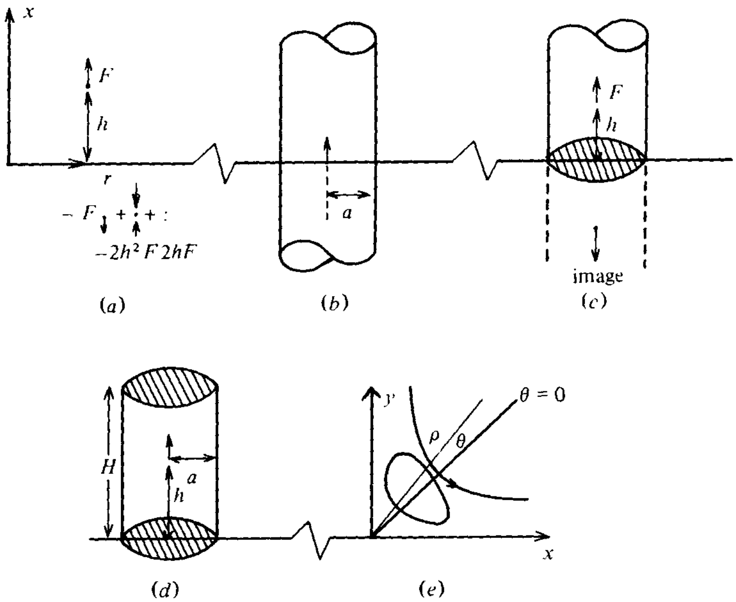

FIGURE 1. Illustrations of the different geometries and notation used in the paper: (*a*) half-space; (*b*) infinite cylinder; (*c*) semi-infinite cylinder; (*d*) finite cylinder; (*e*) corner eddies.

and filtration of colloidal-sized particles and the flow fields generated by micro-organisms between a microscope slide and coverslip. The last-mentioned topic is the one of particular interest to us, as current hydrodynamical theory has been unable to explain the flow fields due to sessile organisms observed under a microscope (see, e.g., Lunec 1975). Recent observations by Sleigh & Barlow (1976) on *Vorticella* shows that this organism can generate an axisymmetric vortex. Closer observation suggests that the size and shape of the vortex is very clearly determined by the geometry and dimensions of the container. It can be shown by using the ideas of Liron & Mochon (1976) that for a microscope slide and coverslip close together the far field for a point force (i.e. the sessile organism) parallel to the slide reduces to a two-dimensional source-doublet (i.e. results for a Hele–Shaw cell), which has circular streamlines. Flow fields around motile organisms appear to be much better understood, especially ciliates (Lighthill 1952; Blake 1973; Keller & Wu 1977) where the far field is a three-dimensional source-doublet.

Of particular relevance to this paper is the classic work of Rayleigh (1920), Dean & Montagnon (1949) and Moffatt (1964) on flow in a corner. Moffatt showed the existence of an infinite set of eddies in the corner when the angle subtended by the plane walls is less than 146° and the driving flow is asymmetric about the bisecting plane. His results for the case when the walls meet at an angle of 90° are applicable to the case of flow in the corners of the finite and semi-infinite cylinders considered in this paper. We obtain what we may call *interior* viscous toroidal eddies of differing sizes depending on the radius and length of the cylinder as well as the Moffatt *corner* eddies mentioned above. For an infinite and semi-infinite cylinder we obtain an infinite set of *interior* eddies; the eddies alternate in sign with their magnitude decreasing exponentially as we move away from the driving singularity. This result compares with Moffatt's example when the angle between the planes is zero. For a finite cylinder, the number of interior eddies depends on the ratio of the length to radius. In the case of the finite cylinders we call the eddies adjacent to the stokeslet a *primary* eddy and other interior eddies we classify as *secondary* eddies. Several examples are considered at the end of the paper.

Recent papers by Fitzgerald (1972), Davis & O'Neill (1977), Yoo & Joseph (1978), Liu & Joseph (1978) and Liron & Shahar (1978) have shown the existence of viscous eddies in confined geometries.

In the next four sections, we will investigate the flow fields (streamlines) for the following axisymmetric cases: (*a*) half-space, (*b*) infinite cylinder, (*c*) semi-infinite cylinder and (*d*) finite cylinders. The respective geometries are shown in figure 1. The *stokeslet* is the fundamental singularity of the Stokes flow equations:

$$\left.\begin{aligned} \nabla p &= \mu\nabla^2\mathbf{u} + \mathbf{F}\delta(\mathbf{x}), \\ \nabla.\mathbf{u} &= 0. \end{aligned}\right\}. \tag{2}$$

Here p is the pressure, $\mathbf{u}$ the Cartesian velocity vector, $\mathbf{F}\delta(\mathbf{x})$ a point force at the origin where $\delta(\mathbf{x})$ is the three-dimensional Dirac delta function. Equation (2) will be solved, subject to the usual no-slip conditions, in the geometries shown in figure 1. The solution will consist of the fundamental singularity plus the additional complementary solution for the required geometry. For the half-space fluid, the image system (outside the flow field) will contain stokeslets, Stokes-doublets and source-doublets. It is also of interest to calculate the streamlines due to these singularities in an infinite cylinder.

The mathematical analysis, in the next sections, will involve the solution of the following axisymmetric equation, in cylindrical co-ordinates, for the complementary stream function ψ,

$$D^4\psi = 0, \tag{3a}$$

where

$$D^2 = \frac{\partial^2}{\partial r^2} - \frac{1}{r}\frac{\partial}{\partial r} + \frac{\partial^2}{\partial x^2}. \tag{3b}$$

Here, the axial velocity u and radial velocity v are defined by

$$u = \frac{1}{r}\frac{\partial\psi}{\partial r}, \quad v = -\frac{1}{r}\frac{\partial\psi}{\partial x}. \tag{3c}$$

Methods of solution are *via* Fourier transforms and Fourier–Bessel series.

2. Half-space problem

The solution to the problem depicted in figure 1 (*a*) of a vertical point force above a plane no-slip boundary is well known (Lorentz 1907; Oseen 1928). An explicit expression for the velocity and pressure field in terms of the stokeslet in the fluid and the image system comprising a stokeslet, Stokes-doublet and a source doublet can be found in Blake (1971) and is also illustrated in figure 1 (*a*).

In terms of the stream function ψ (scaled with respect to $8\pi\mu$), the solution for the case when $h = 1$ (this is the only length scale, so without loss of generality we can set it equal to 1) is

$$\psi = \frac{r^2}{[r^2+(x-1)^2]^{\frac{1}{2}}} - \frac{r^2}{[r^2+(x+1)^2]^{\frac{1}{2}}} - \frac{2r^2x}{[r^2+(x+1)^2]^{\frac{3}{2}}}. \tag{4}$$

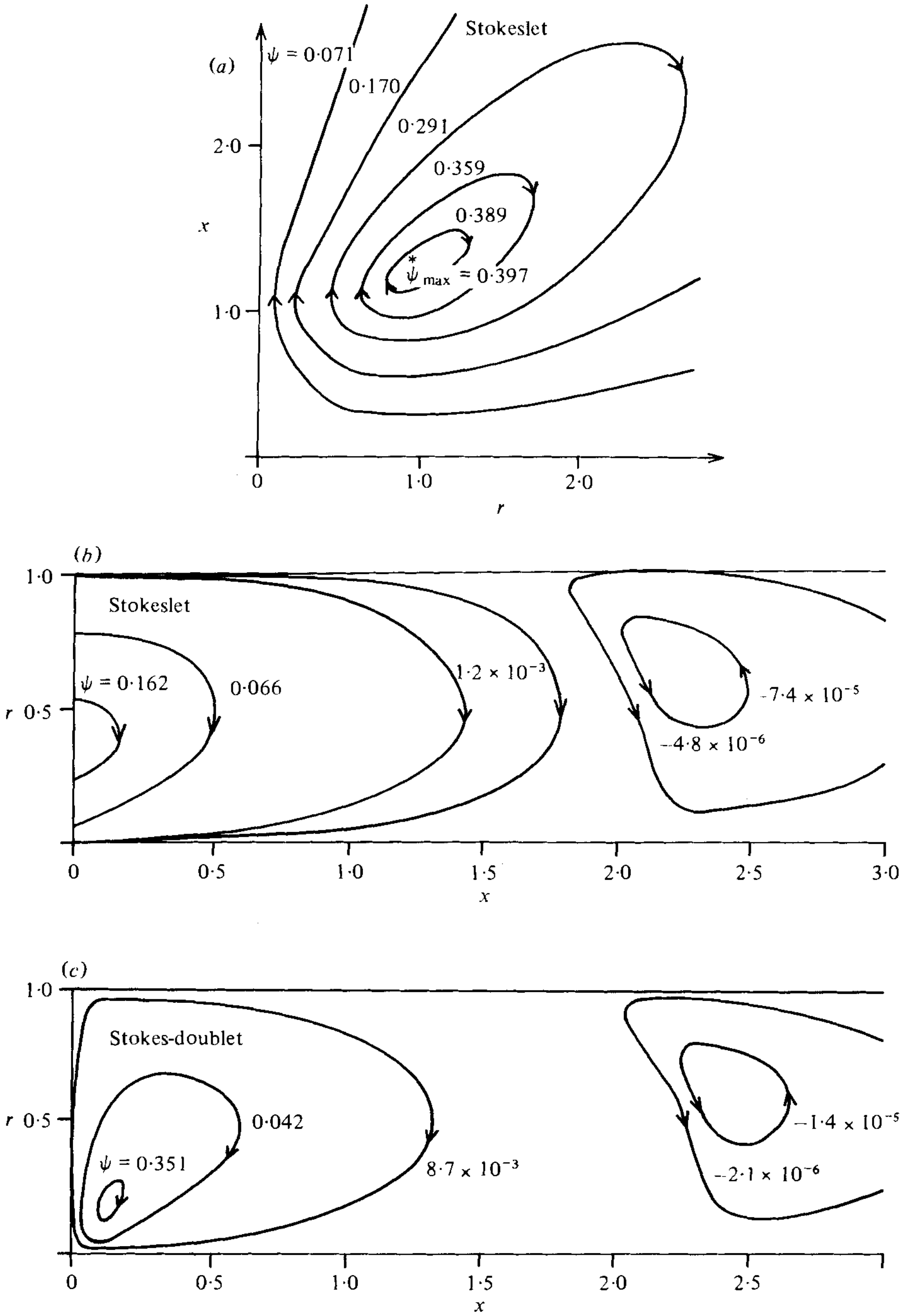

FIGURE 2 (a, b, c). For legend see next page.

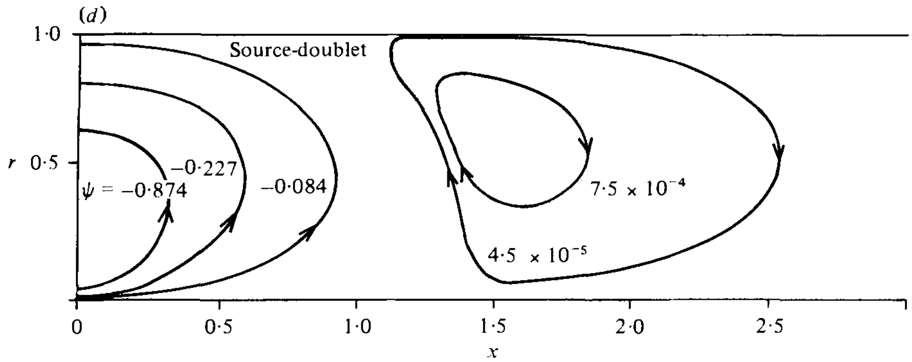

FIGURE 2. (a) Axisymmetric streamlines in a half-space due to a vertical point force. The first few of the infinite set of toroidal eddies found in an infinite cylinder owing to the following singularities are shown in (b) due to a stokeslet, in (c) a Stokes-doublet and in (d) a source-doublet.

The first and second terms are stokeslets within the half-space and at the image point respectively while the third term is a combination of a Stokes-doublet and a source-doublet. The resulting streamlines are shown in figure 2(a). The maximum value of ψ occurs at $r = 1{\cdot}056$ and $x = 1{\cdot}248$ and has the value $\psi_{max} = 0{\cdot}397$. An acoustical analogy discussed by Lighthill (1978, figure 83) has similar streamlines to those shown in figure 2(a).

3. Infinite cylinder

Our eventual aim is to obtain a semi-analytic solution for a stokeslet in a semi-infinite cylinder. With a knowledge of the image system for the half-space problem it is prudent for us to obtain the solutions for a stokeslet, Stokes-doublet and a source-doublet in an infinite cylinder in terms of the stream function ψ.

(a) *Stokeslet*

As outlined in the introduction, the method of analysis will be to find the complementary solution to the fundamental singularity in the particular geometry, in this case, the infinite cylinder. Thus the stream function ψ will consist of two parts:

$$\psi = \psi_0 + \psi_1, \tag{5a}$$

where ψ_0 is the stream function for a stokeslet at the origin in an infinite fluid,

$$\psi_0 = r^2/[x^2+r^2]^{\frac{1}{2}} \tag{5b}$$

and ψ_1 is the complementary function which to be calculated. The no-slip boundary conditions require that

$$\psi = \partial\psi/\partial r = 0 \quad \text{on} \quad r = a. \tag{6}$$

A method of solution is to use Fourier transforms. To avoid branch points, we need to include the transform of ψ_0 in the inverse Fourier transform. We then find the solution for ψ is

$$\psi(r,x) = \sum_{\substack{n=-\infty \\ n\neq 0}}^{\infty} K_n(r)\exp[-\alpha_n|x|/a], \tag{7a}$$

where

$$K_n(r) = A_n r 2 J_0(\alpha_n r/a) + B_n r J_1(\alpha_n r/a), \tag{7b}$$

$$A_n = \frac{\pi}{2aJ_1^2}(2J_1 Y_0 - \alpha_n(J_0 Y_0 + J_1 Y_1)) \tag{7c}$$

and

$$B_n = -1/J_1^2, \tag{7d}$$

with the α_n satisfying the following equation

$$\alpha_n(J_0^2(\alpha_n) + J_1^2(\alpha_n)) = 2J_0(\alpha_n) J_1(\alpha_n), \quad \mathrm{Re}\,(\alpha_n) > 0. \tag{7e}$$

It is easy to show that $\alpha_{-n} = \bar{\alpha}_n$, the complex conjugate. In (7c) and (7d) the Bessel function arguments are α_n. Because of the properties of the Bessel functions (7a) may be expressed as

$$\psi(r,x) = 2\,\mathrm{Re} \sum_{n=1}^{\infty} K_n(r) \exp[-\alpha_n|x|/a]. \tag{8}$$

The first thirty roots α_n of (7e) are listed in Friedmann, Gillis & Liron (1968). We observe that ψ decays exponentially with axial distance x. We also observe that, since the α_n are complex, in the far field where α_1 dominates there must exist closed periodic eddies. The wavelength of the eddies in the far field is $\lambda = \pi a/\mathrm{Im}\,(\alpha_1) \sim 2{\cdot}15a$. Streamlines for ψ are shown in figure 2(b). Indentical results to this have been obtained by Liron & Shahar (1978).

(b) *Stokes-doublet*

The stream function ψ on this case can be obtained trivially by taking the derivative in the x direction. We obtain

$$\psi(r,x) = 2\,\mathrm{Re} \sum_{n=1}^{\infty} \frac{\alpha_n}{a} \mathrm{sgn}\,(x)\,(A_n r^2 J_0(\alpha_n r/a) + B_n r J_1(\alpha_n r/a)) \exp[-\alpha_n|x|/a], \tag{9}$$

where A_n and B_n are defined in (7c) and (7d) respectively and α_n in (7e). Streamlines are shown in figure 2(c).

(c) *Source-doublet*

Using an identical procedure to that employed in obtaining the stokeslet, we obtain the following expression for ψ in the case of a source-doublet:

$$\psi(r,x) = 2\,\mathrm{Re} \sum_{n=1}^{\infty} (C_n r^2 J_0(\alpha_n r/a) + D_n r J_1(\alpha_n r/a)) \exp(-\alpha_n|x|/a), \tag{10a}$$

where

$$C_n = -\alpha_n/a^3 J_1^2, \tag{10b}$$

$$D_n = \frac{\pi}{2a^2 J_1^2}[\alpha_n^2(J_0 Y_0 + J_1 Y_1) - 2\alpha_n J_0 Y_1] \tag{10c}$$

and α_n satisfies (7e). Streamlines are shown in figure 2(d).

4. Semi-infinite cylinder

In principle we can obtain an analytic solution for the semi-infinite cylinder problem by using all eigenfunctions and suitable transformations on the boundaries. However, this involves lengthy and tedious algebraic manipulation. A much simpler method is to approximate the boundary conditions on the plane boundary at $x = 0$ in figure 1(c).

With a knowledge of the solution for a stokeslet in an infinite cylinder from the previous section, we use the following analytic expression to represent the solution in the semi-infinite cylinder ($x \geqslant 0$),

$$\psi(r,x) = \sum_{\substack{n=-\infty \\ n\neq 0}}^{\infty} [K_n(r)(\exp[-\alpha_n|x-h|/a] - \exp[-\alpha_n(x+h)/a]) \\ + E_n\phi_n(r)\exp[-\alpha_n(x+h)/a], \tag{11a}$$

where $K_n(r)$ is defined in (7b) and

$$\phi_n(r) = r^2 J_0(\alpha_n r/a) - ar\, J_0(\alpha_n)\, J_1(\alpha_n r/a)/J_1(\alpha_n). \tag{11b}$$

The eigenfunction $\phi_n(r)$ and equation (7e) for α_n come from the boundary conditions on $r = a$. The stokeslet is located at $(0, h)$ and the complementary singularities at $(0, -h)$. The boundary conditions on $x = 0$ are

$$\psi = \frac{\partial\psi}{\partial x} = 0. \tag{12}$$

The E_n are obtained by a least squares approximation of these boundary conditions (12). We define

$$\mathscr{E} = \int_0^a \frac{1}{r}\left(\psi\bigg|_0^2 + \frac{\partial\psi}{\partial x}\bigg|_0^2\right) dr \tag{13a}$$

and as usual we require that

$$\frac{\partial\mathscr{E}}{\partial E_k} = 0 \quad k = \pm 1, \pm 2, \pm 3, \ldots. \tag{13b}$$

Since the stream function ψ is real, we may assume that $E_{-n} = \bar{E}_n$, the overbar implying the complex conjugate. This now allows us to reduce the summation of (11a) to the positive integers.

Using the summation convention, application of the condition (13b) to (13a) yields the following infinite matrix for C_n

$$F_{kn}E_n = P_k \quad k = \pm 1, \pm 2, \pm 3, \ldots, \tag{14a}$$

where
$$F_{kn} = \exp[-(h/a)(\alpha_k + \alpha_n)]\left(1 + \frac{\alpha_k\alpha_n}{a^2}\right)\int_0^a \frac{1}{r}\phi_k\phi_n\, dr \tag{14b}$$

and
$$P_k = \sum_{\substack{n=-\infty \\ n\neq 0}}^{\infty} \exp[-(h/a)(\alpha_k + \alpha_n)]\frac{\alpha_n\alpha_k}{a^2}\int_0^a \frac{1}{r}\phi_k K_n\, dr. \tag{14c}$$

The integrals in (14b) and (14c) can be evaluated in terms of Bessel functions of the first kind. The infinite set of linear equations is truncated to a $2N \times 2N$ system. However, we can reduce the system to a $N \times N$ set by making use of the following relationships,

$$F_{-k-n} = \overline{F_{kn}}, \quad F_{-kn} = \overline{F_{k-n}}, \quad P_{-k} = \overline{P_k}, \quad k = 1, 2, 3, \ldots. \tag{15}$$

On substitution of these values of E_n into (11a) the stream function ψ can be obtained as a function of position.

In the calculations we used $N = 30$ and found the E_n to decay exponentially with n. As expected, the maximum value of ψ occurs on the plane $x = h$ and has magnitude $O(1)$. The approximated value of the stream function on the plane boundary is $O(10^{-6})$.

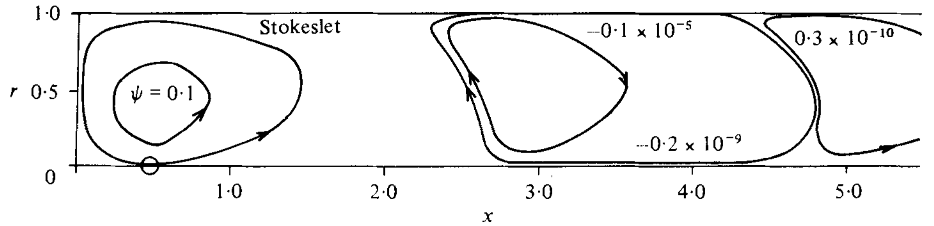

FIGURE 3. Toroidal eddies found in a semi-infinite cylinder for $h = 0{\cdot}5$.

In figure 3, an example of the streamlines for a semi-infinite cylinder is illustrated. In the far field an infinite set of eddies of alternating sign is obtained similar to the infinite cylinder case. The number of *interior* eddies between the stokeslet and plane no-slip boundary is determined by the value of h/a. Moffat *corner* eddies are obtained near the junction of the cylindrical and plane boundaries.

5. Finite cylinder

The problem of a stokeslet in a finite cylinder is solved by using two different methods. In the first approach we use an extension of the semi-analytic least squares approach of the last section while in the second we use a finite difference approximation to the stream function equations. In the third part of this section we briefly discuss Moffatt corner eddies as they are applicable to a finite cylinder.

(i) *Semi-analytic least squares method*

Again we suppose the stokeslet is located at $(0, h)$ and that boundary conditions (6) apply on $r = a$ and (12) apply on $x = 0$ and H (see figure 1*d*). In this case we use the following expression for ψ $(0 \leqslant x \leqslant H)$,

$$\psi(r,x) = \sum_{\substack{n=-\infty \\ n \neq 0}}^{\infty} [K_n(r)\exp[-\alpha_n|x-h|/a] + \phi_n(r)\,(G_n \exp[-\alpha_n x/a] + H_n \exp[\alpha_n(x-H)/a])], \tag{16}$$

where K_n is defined in (7*b*), ϕ_n in (11*b*) and α_n in (7*e*). The G_n and H_n are obtained by approximating the boundary conditions on $x = 0$ and H. For the case of the finite cylinder, we define

$$\mathscr{E} = \int_0^a \frac{1}{r}\left(\psi\Big|_0^2 + \frac{\partial\psi}{\partial x}\Big|_0^2 + \psi\Big|_H^2 + \frac{\partial\psi}{\partial x}\Big|_H^2\right) dr, \tag{17a}$$

where the subscript indicates where the stream function or its derivative is evaluated. In this case we require that

$$\frac{\partial\mathscr{E}}{\partial G_k} = 0 \quad \text{and} \quad \frac{\partial\mathscr{E}}{\partial H_k} = 0 \quad k = \pm 1, \pm 2, \ldots. \tag{17b}$$

We assume that $G_{-n} = \overline{G_n}$ and $H_{-n} = \overline{H_n}$.
In this case we obtain

$$R_{kn}\, G_n + S_{kn}\, H_n = Q_k$$

and

$$S_{kn}\, G_n + R_{kn}\, H_n = T_k \quad k, n = \pm 1, \pm 2, \ldots, \tag{18a}$$

where $$R_{kn} = \left(1+\frac{\alpha_k\alpha_n}{a^2}\right)(1+\exp[-H(\alpha_k+\alpha_n)/a])\int_0^a \frac{1}{r}\phi_k\phi_n\,dr, \tag{18b}$$

$$S_{kn} = \left(1-\frac{\alpha_k\alpha_n}{a^2}\right)(\exp[-\alpha_k H/a]+\exp[-\alpha_n H/a])\int_0^a \frac{1}{r}\phi_k\phi_n\,dr, \tag{18c}$$

$$Q_k = -\sum_{\substack{n=-\infty\\ n\neq 0}}^{\infty}\left\{\left(1-\frac{\alpha_k\alpha_n}{a^2}\right)\exp[-\alpha_n h/a] + \left(1+\frac{\alpha_k\alpha_n}{a^2}\right)\exp[(-H(\alpha_k+\alpha_n)+h\alpha_n)/a]\right\}\int_0^a \frac{1}{r}\phi_k K_n\,dr, \tag{18d}$$

$$T_k = -\sum_{\substack{n=-\infty\\ n\neq 0}}^{\infty}\left\{\left(1-\frac{\alpha_k\alpha_n}{a^2}\right)\exp[-\alpha_n(H-h)/a] + \left(1+\frac{\alpha_k\alpha_n}{a^2}\right)\exp[-(h\alpha_n+H\alpha_k)/a]\right\}\int_0^a \frac{1}{r}\phi_k K_n\,dr. \tag{18e}$$

If we add and subtract the equations in (18*a*) we obtain two sets of linear equations

$$A_{kn}\theta_n = U_k, \quad B_{kn}\omega_k = V_k, \tag{19a}$$

where
$$\left.\begin{aligned} A_{kn} &= R_{kn}+S_{kn}, & B_{kn} &= R_{kn}-S_{kn},\\ U_k &= Q_k+T_k, & V_k &= Q_k-T_k,\\ \theta_n &= G_n+H_n, & \omega_n &= G_n-H_n. \end{aligned}\right\} \tag{19b}$$

By this manipulation we can reduce the size of the truncated matrix (for N positive terms in the series) from a $4N\times 4N$ to a $2N\times 2N$ system. As before for the semi-infinite cylinder by using the complex conjugate of matrix elements, the size of the matrix can be reduced to a $N\times N$ system. We then solve (19*a*) for the complex values of θ_n and ω_n and hence G_n and H_n which are then substituted into (16) to obtain the streamlines.

(ii) *Finite difference approximation*

Streamlines due to a stokeslet in a finite cylinder were also obtained by a finite difference approximation (FDA). As in the case of the infinite cylinder example we split the stream function into two parts,

$$\psi = \psi_0+\psi_1, \tag{20a}$$

where ψ_0 is the solution for a stokeslet in an infinite fluid and ψ_1 is the complementary solution. We obtain ψ_1 by using a FDA. In this example the stokeslet is located at $(0,h)$ so ψ_0 is defined as follows,

$$\psi_0 = \frac{r^2}{[r^2+(x-h)^2]^{\frac{1}{2}}}. \tag{20b}$$

The complementary stream function ψ_1 satisfies the axisymmetric stream function in cylindrical co-ordinates defined in (3*a*) and (3*b*). The boundary conditions on ψ_1 are

$$\psi_1 = -\psi_0 \quad\text{and}\quad \frac{\partial\psi_1}{\partial x} = -\frac{\partial\psi_0}{\partial x} \quad\text{on}\quad x = 0, H \tag{21a}$$

and $$\psi_1 = -\psi_0 \quad\text{and}\quad \frac{\partial\psi_1}{\partial r} = -\frac{\partial\psi_0}{\partial r} \quad\text{on}\quad r = a. \tag{21b}$$

Because of symmetry on the x-axis, we also require that

$$\psi_1 = 0 \quad \text{and} \quad \frac{\partial u}{\partial r} = 0 \quad \text{on} \quad r = 0, \tag{21c}$$

where u is the axial velocity and is defined in (3c).

In the FDA we solve the coupled equations,

$$D^2\phi = 0 \tag{22a}$$

and

$$D^2\psi = \phi = -r\omega, \tag{22b}$$

where ϕ is related to the vorticity ω by the expression on the right-hand side of (22b). As with the stream function ψ, we divide ϕ into the stokeslet ϕ_0 and complementary component ϕ_1:

$$\phi = \phi_0 + \phi_1, \tag{23a}$$

where

$$\phi_0 = \frac{-2r^2}{(r^2+(x-h)^2)^{\frac{3}{2}}}. \tag{23b}$$

We solve (22a) and (22b) by the method of successive over-relaxation (SOR). The discretization for nodal elements $\phi_{i,j} = \phi(r_i, x_j)$ and $\psi_{i,j} = \psi(r_i, x_j)$ ($2 \leqslant i \leqslant M-1$; $2 \leqslant j \leqslant N-1$) used in the computations is as follows,

$$\phi_{i,j} = \phi_{i,j} + \frac{\Omega}{\gamma_i}\left[\frac{r_i}{r_{i+\frac{1}{2}}}\phi_{i+1,j} - \gamma_i\phi_{i,j} + \frac{r_i}{r_{i-\frac{1}{2}}}\phi_{i-1,j} + \beta^2\phi_{i,j+1} + \beta^2\phi_{i,j-1}\right] \tag{24a}$$

and

$$\psi_{i,j} = \psi_{i,j} + \frac{\Omega}{\gamma_i}\left[\frac{r_i}{r_{i+\frac{1}{2}}}\psi_{i+1,j} - \gamma_i\psi_{i,j} + \frac{r_i}{r_{i-\frac{1}{2}}}\psi_{i-1,j} + \beta^2\psi_{i,j+1} + \beta^2\psi_{i,j-1} - (\Delta r)^2\phi_{i,j}\right], \tag{24b}$$

where $\Delta x = H/(N-1)$, $\Delta r = a/(M-1)$, $\beta = \Delta x/\Delta r$, Ω is the relaxation parameter and γ_i is the normalization parameter defined as

$$\gamma_i = r_i\left(\frac{1}{r_{i+\frac{1}{2}}} + \frac{1}{r_{i-\frac{1}{2}}}\right) + 2\beta^2. \tag{24c}$$

The boundary conditions for ψ_1 can be obtained from (21a, b, c). However we have to approximate the boundary conditions for ϕ_1, except on $r = 0$ where it is identically equal to zero. Methods for overcoming this difficulty are discussed in Roache (1972). A Taylor series expansion about the boundary points is used to the required accuracy to derive the approximation for ϕ. We use the simplest first-order approximation in our calculations, as follows:

$$\phi_{i1} = \frac{2\psi_{i2}}{r_i(\Delta x)^2} \quad \text{on} \quad x = 0, \tag{25a}$$

$$\phi_{iN} = \frac{2\psi_{i,N-1}}{r_i(\Delta x)^2} \quad \text{on} \quad x = H \tag{25b}$$

and

$$\phi_{Mj} = \frac{2r_i^2\psi_{M-1,j}}{r_{i+\frac{1}{2}}r_{i-\frac{1}{2}}(\Delta r)^2} \quad \text{on} \quad r = a. \tag{25c}$$

In these expressions we are using the definitions of ψ in (20a) and ϕ in (23a) so that a minor rearrangement is needed to obtain the boundary approximations for ϕ_1. One

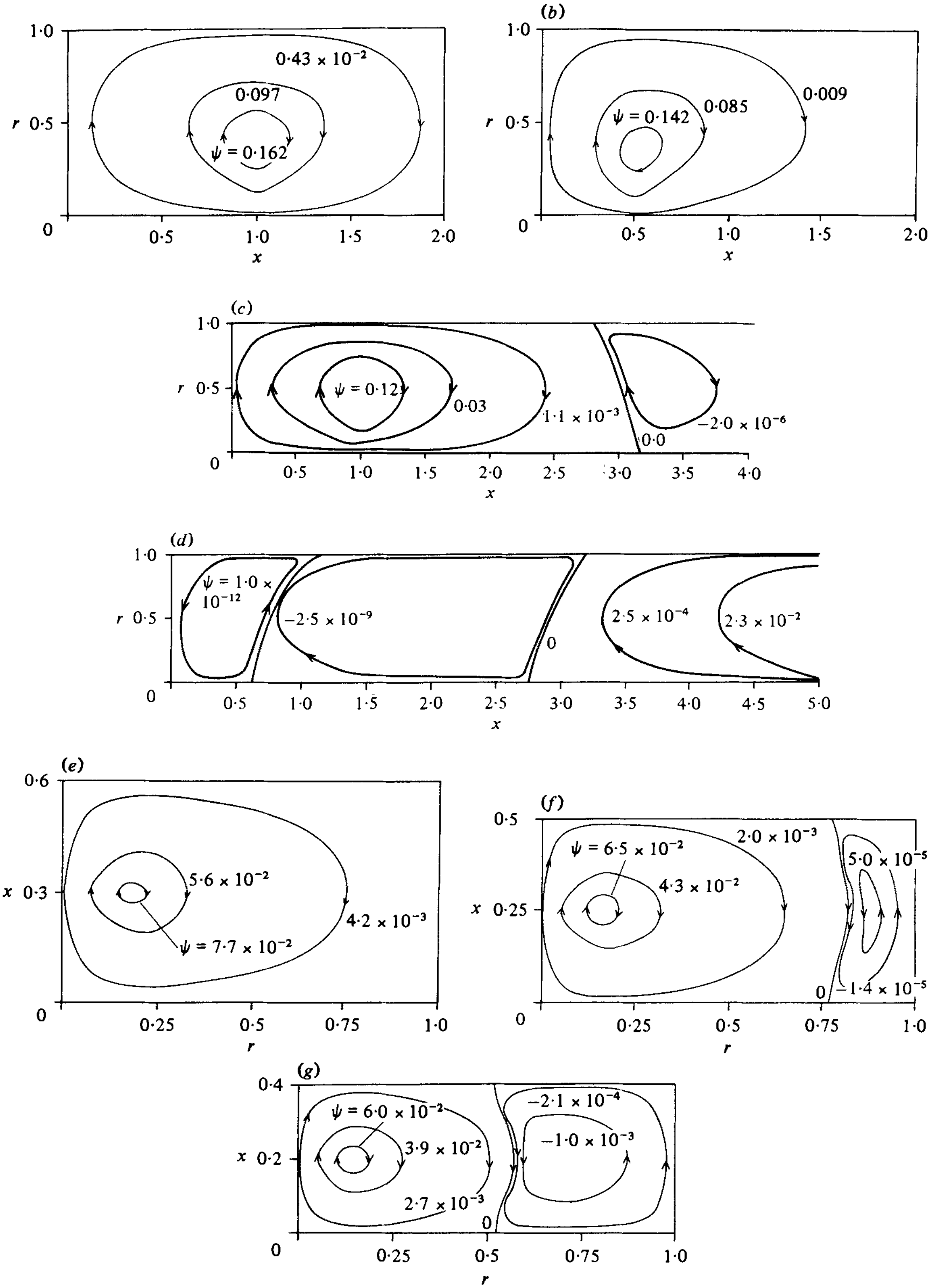

FIGURE 4. The finite number of toroidal interior eddies found in a finite cylinder of varying length and stokeslet location. (a) $h = 1{\cdot}0, H = 2{\cdot}0$; (b) $h = 0{\cdot}5, H = 2{\cdot}0$; (c) $h = 1{\cdot}0, H = 4{\cdot}0$; (d) $h = 5{\cdot}0, H = 10{\cdot}0$ (only half of the cylinder is shown): (e) $h = 0{\cdot}3, H = 0{\cdot}6$; (f) $h = 0{\cdot}25, H = 0{\cdot}5$; (g) $h = 0{\cdot}2, H = 0{\cdot}4$.

difficulty occurs, in that our initial estimates for ϕ_1 on the boundary are generally only accurate to $O(1)$. We overcome this by using under-relaxation techniques on the iterates for boundary values of ϕ_1. For example in the case of $x = 0$, we use

$$\phi_{i1}^{n} = \phi_{i1}^{n-1} + \alpha \left[\frac{2\psi_{i2}^{n-1}}{r_i(\Delta x)^2} - \phi_{i1}^{n-1} \right]. \tag{26}$$

Another minor difficulty was in obtaining estimates for the corner values of ϕ (i.e. ϕ_{M1} and ϕ_{MN}). Two approaches were used to obtain these values (*a*) by extrapolation from the nearby boundary values of ϕ and (*b*) by analytical methods based on Moffatt's (1964) paper which showed that both values are identically zero. Because of the importance of the corner-eddies and the values of corner vorticity the germane ideas of Moffatt's paper will be reproduced in the next part of this section. The SOR numerical solution of the problem produces eddies in the corner but it cannot be expected to reproduce accurately the complexity of the streamlines. Furthermore the SOR approach cannot be expected to calculate the stream function accurately for long cylinders ($H/a \geqslant 4{\cdot}0$) because of the exponential decrease in the stream function, unless we have an extremely fine mesh. However, in the case of squat cylinders ($H/a < 1{\cdot}0$) the series solution is not desirable because of the slow convergence near the singularity, so here the FDA is used.

In the regions of joint validity the least squares ($N = 15, 30$) and SOR results are identical within the designed accuracy. In the SOR computations the optimal values of Ω and α depend on h/a and H/a and the number of grid points employed ($M = 11$–41, $N = 21$–81). In figure 4(*a*) only one primary symmetric *interior* eddy occupies the entire cylinder with the exception of the corner eddies (marked with an asterisk on figure 4(*a*)). In figure 4(*b*) the streamlines are skewed because the stokeslet is located closer to one end. In figure 4(*c*) we see the existence of two large *interior* eddies (primary and secondary) while in figure 4(*d*) five interior eddies have developed (because of the length of the cylinder and symmetry only half of it is shown in the diagram). In the last three diagrams of figure 4, the emergence of eddies in the radial direction is illustrated for squat cylinders. In figure 4(*e*), no secondary eddies exist, but in figure 4(*f*) we observe that a small interior eddy has appeared near the outer cylindrical boundary. In figure 4(*g*) a substantial secondary eddy has developed of similar linear dimensions to the primary eddy.

(iii) *Corner (Moffatt) eddies*

One of the cases Moffatt (1964) studied was the flow field generated in the corner between two planes due to an asymmetric outer flow field. Near the corners in this current problem the boundaries may be approximated by two planes at 90° to each other (corresponds to $\alpha = 45°$ in Moffatt's paper). The geometry of the problem is illustrated in figure 1*e*). We define θ as the angle from bisector of the two planes (hence $\theta = \pm 45°$ corresponds to the no-slip boundaries) and $\rho = (x^2+y^2)^{\frac{1}{2}}$, the local radial co-ordinate.

Near the corner the stream function can be adequately represented by the first term in an infinite series,

$$\psi \sim A' \left(\frac{\rho}{\rho_0}\right)^{\lambda_1} [\cos \lambda_1 \theta \cos \tfrac{1}{4}\pi(\lambda_1 - 2) - \cos (\lambda_1 - 2)\theta \cos \tfrac{1}{4}\pi \lambda_1], \tag{27a}$$

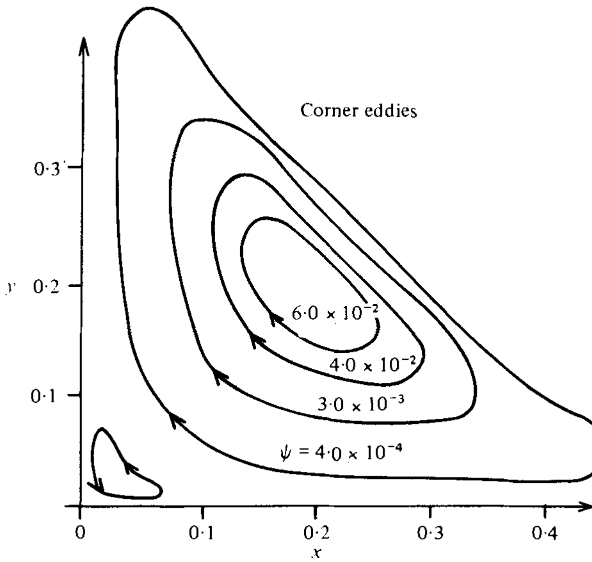

FIGURE 5. The corner eddy structure.

where ρ_0 is a scale length and λ_1 is the smallest eigenvalue of the transcendental equation

$$\sin\tfrac{1}{2}\pi\mu = -\mu, \quad \text{where} \quad \mu = \lambda_1 - 1. \tag{27b}$$

This equation can be easily solved using Newton's method, yielding

$$\lambda_1 = 3{\cdot}7396 + 1{\cdot}1908i.$$

Now since ϕ is directly proportional to the vorticity it must behave like $O(\rho^{\lambda_1-2})$ in the corners. As the Re (λ_1) is greater than 2, ϕ must tend to zero at these points. Therefore we have equated ϕ to zero in the corners in the numerical solution of the equations.

Graphs of the corner eddy structure are shown in figure 5 (illustrative only, not same scale as other diagrams). We observe the exponential decrease in the magnitude of the stream function for the corner eddies. The obvious comment should be made that the size of the corner eddies is very much less than that of the interior eddies.

The author acknowledges the many helpful comments made on this work by Dr Nadav Liron and Dr Frank deHoog.

REFERENCES

ADEROGBA, K. 1976 On stokeslets in a two-fluid space. *J. Engng Math.* **10**, 143–151.

BLAKE, J. R. 1971 A note on the image system for a stokeslet in a no-slip boundary. *Proc. Camb. Phil. Soc.* **70**, 303–310.

BLAKE, J. 1973 A finite model for ciliated micro-organisms. *J. Biomech.* **6**, 133–140.

DAVIS, A. M. J. & O'NEILL, M. E. 1977 The development of viscous wakes in a Stokes flow when a particle is near a large particle. *Chem. Engng Sci.* **32**, 899–906.

DEAN, W. R. & MONTAGNON, P. E. 1949 On the steady motion of a viscous liquid in a corner. *Proc. Camb. Phil. Soc.* **45**, 389–394.

FITZGERALD, J. M. 1972 Plasma motions in capillary flow. *J. Fluid Mech.* **51**, 463–476.

FRIEDMANN, M., GILLIS, J. & LIRON, N. 1968 Laminar flow in a pipe at low and moderate Reynolds numbers. *Appl. Sci. Res.* **19**, 426–438.

HAPPEL, J. & BRENNER, H. 1965 *Low Reynolds Number Hydrodynamics*. Englewood Cliffs, N.J.: Prentice-Hall.

KELLER, S. R. & WU, T. Y. 1977 A porous prolate-spheroidal model for ciliated micro-organisms. *J. Fluid Mech.* **80**, 259–278.

LIGHTHILL, M. J. 1952 On the squirming motions of nearly spherical deformable bodies through liquids at very small Reynolds numbers. *Communs pure appl. Math.* **5**, 109–118.

LIGHTHILL, J. 1978 *Waves in Fluids*. Cambridge University Press.

LIRON, N. & MOCHON, S. 1976 Stokes flow for a stokeslet between parallel flat plates. *J. Engng Math.* **10**, 287–303.

LIRON, N. & SHAHAR, R. 1978 Stokes flow due to a stokeslet in a pipe. *J. Fluid Mech.* **86**, 727–744.

LIU, C. H. & JOSEPH, D. D. 1978 Stokes flow in conical trenches. *SIAM J. Appl. Math.* **34**, 286–296.

LORENTZ, H. A. 1907 *Abhandlungen über theoretische Physik* **1**, 23–32. Leipzig.

LUNEC, J. 1975 Fluid flow induced by smooth flagella. In *Swimming and Flying in Nature* (ed. T. Y. Wu, C. J. Brokaw & C. Brennen), pp. 143–160. N.Y.: Plenum.

MOFFATT, H. K. 1964 Viscous and resistive eddies near a sharp corner. *J. Fluid Mech.* **18**, 1–18.

OSEEN, C. W. 1928 *Hydrodynamik*. Leipzig.

RAYLEIGH, LORD 1920 Steady motion in a corner of a viscous fluid. *Sci. Papers* **6**, 18–21.

ROACHE, P. J. 1972 *Computational Fluid Dynamics*. Albuquerque, N.M.: Hermosa.

SLEIGH, M. A. & BARLOW, D. 1976 Collection of food by *Vorticella*. *Trans. Am. Micros. Soc.* **95**, 482–486.

YOO, J. Y. & JOSEPH, D. D. 1978 Stokes flow in a trench between concentric cylinders. *SIAM J. Appl. Math.* **34**, 247–285.